Front. Electr. Electron. Eng. China 2010, 5(2): 224–228
DOI 10.1007/s11460-010-0016-z

RESEARCH ARTICLE

Hongxia HUANG, Lin LI, Zhibin ZHAO

A fast algorithm for computing electromagnetic fields of a thin wire current source inside lossy ground

Abstract In this paper, a fast algorithm is presented to compute the electromagnetic fields of a thin wire current source inside lossy ground. The modified image method is used to evaluate the Sommerfeld integrals, and the fast multipole method (FMM) is utilized for solving the governing electric field integral equation (EFIE). The validation of the proposed algorithm is performed by comparing the results with that of using method of moment (MoM). The numerical example shows the flexibility, efficiency and accuracy of this algorithm.

Keywords modified image theory, lossy ground, fast multipole method (FMM)

1 Introduction

In the past decades, much attention has been paid to the problem of the interaction between lightning electromagnetic fields and the grounding grids of substations or overhead transmission lines. This had led to the formulations of different reliable models based on the antenna theory and thin wire approximation. All these models require accurate evaluations of the lightning electromagnetic fields produced by the thin wire current sources above or below ground taking into account the effect of ground conductivity. Unfortunately, the presence of the lossy ground in the model implies the computation of the slowly converging Sommerfeld integrals, which makes the performance of the algorithms prohibitive in terms of large computation time, especially for large grounding grids or long transmission lines. As a result, many simplified approaches have been developed to overcome the above problem [1–4], and some efficient algorithms have been proposed to evaluate the exact expressions in order to test the validity of the approximate formulas [5,6]. However, a large amount of computation is still required because the inversion of a fully dense matrix is required at each frequency. Fast multipole method (FMM) provides an efficient way for the numerical convolution of the Green's function for the Helmholtz equation iterative solution of boundary-integral equations [7–9]. It employs iterative techniques such as conjugate gradient method or the bi-conjugate gradient method to solve the linear algebraic equations. The method reduces the computational complexity of the convolution from $O(N^2)$ to $O(N^{1.5})$, where N is the discretization dimensionality of the problem. By implementing a multilevel FMM, the complexity can be further reduced to $O(N\lg N)$. However, the key of this method is to expand $\mathrm{e}^{-\mathrm{i}kR}/R$ item (k is the wave number, R is the distance between the observation point and source point), and electric field integral equation (EFIE) for the lossy ground contains Sommerfeld integrals which are not only composed by $\mathrm{e}^{-\mathrm{i}kR}/R$ but by other items. Therefore, FMM cannot be used to evaluate the underground electromagnetic fields if the Sommerfeld integrals are evaluated directly.

In this paper, modified images are used to replace the ground effect in the calculation of electromagnetic fields produced by the thin wire current sources above or below ground, and FMM is utilized for solving the governing electric field integral equation. The remarkable efficiency in terms of CPU time and flexibility of the developed algorithm makes it possible to evaluate the interaction between lightning electromagnetic fields and grounding grids or overhead transmission lines. For the sake of simplicity, in the computation of this paper only the electromagnetic fields due to a thin wire inside a lossy ground are considered. The limitation of the proposed algorithm is related with the use of modified image theory in order to approximate the Sommerfeld integrals in the lossy half-space problem. This treatment for the Sommerfeld integrals limits the range of applicability of the numerical method to frequencies lower than a few

Received January 24, 2010; accepted February 12, 2010

Hongxia HUANG (✉), Lin LI, Zhibin ZHAO
School of Electrical and Electronic Engineering, North China Electric Power University, Baoding 071003, China
E-mail: hhx_1982@163.com

megahertz. However, this range is suitable for the electromagnetic fields of the typical lightning pulse.

2 Formulation

2.1 Modified image theory

The schematic of the problem is shown in Fig. 1 where a thin wire conductor of infinite conductivity is placed in a lossy ground with conductivity σ, permittivity ε, and permeability μ. The upper half space is the air with permittivity ε_0 and permeability μ_0. The current along the wire conductor is considered to be a line source along the wire axis, by using the thin wire approximation. For the lossy medium half-space problem, the influence of the interface between the air and the ground is taken into account approximately by the modified images [10]. By means of this treatment, the problems are reduced to the calculation of electromagnetic field of thin line current sources in the homogeneous spaces, either soil or air, depending on the positions of the observation point. In order to determine the longitudinal current distribution, it can be considered that the current source and observation point are below the ground. The electric field can be evaluated as field due to current source and its image I'. The image current I' can be calculated by

$$I' = \frac{\mathrm{i}\omega\varepsilon + \sigma - \mathrm{i}\omega\varepsilon_0}{\mathrm{i}\omega\varepsilon + \sigma + \mathrm{i}\omega\varepsilon_0} I = aI, \tag{1}$$

where ω is the angular frequency, a is the coefficient of the image current source.

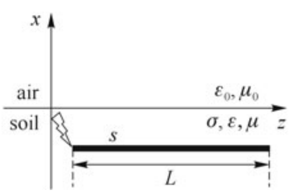

Fig. 1 Schematic of the problem

2.2 Electric field integral equation

The governing EFIE based on the boundary condition of the electric field on the surface of a conductor with a longitudinal current distribution $I_z(r')$ along it can be expressed as follows:

$$\boldsymbol{t}\cdot\boldsymbol{E}^{\mathrm{i}} = -(\boldsymbol{t}\cdot\boldsymbol{E}_1^{\mathrm{s}} + \boldsymbol{t}\cdot\boldsymbol{E}_2^{\mathrm{s}}), \tag{2}$$

where $\boldsymbol{t}$ represents the axial unit vector tangential to the segment surface, $\boldsymbol{E}^{\mathrm{i}}$ is incident field, $\boldsymbol{E}_1^{\mathrm{s}}$ and $\boldsymbol{E}_2^{\mathrm{s}}$ are scattered electric field due to current source and its image, respectively. In this paper, subscript 1 indicates the parameter relative to current source and subscript 2 indicates the parameter relative to its image. The scattered electric field can be expressed as follows:

$$\boldsymbol{t}\cdot\boldsymbol{E}_j^{\mathrm{s}} = \frac{1}{4\pi(\sigma + \mathrm{i}\omega\varepsilon)} \int_l I_z(\boldsymbol{r}_j')G(\boldsymbol{r},\boldsymbol{r}_j')\mathrm{d}z, \quad j = 1,2, \tag{3}$$

where $\boldsymbol{t}$ is the unit vector along the wire axis and tangential to its surface, and $\boldsymbol{r}$ and $\boldsymbol{r}_j'$ are observation and source point vectors, respectively. The Green's function $G(\boldsymbol{r},\boldsymbol{r}_j')$ is defined as

$$G(\boldsymbol{r},\boldsymbol{r}_j') = (\nabla^2 - \gamma^2)\frac{\mathrm{e}^{-\gamma|\boldsymbol{r}-\boldsymbol{r}_j'|}}{|\boldsymbol{r}-\boldsymbol{r}_j'|}, \tag{4}$$

$$\gamma = \sqrt{\mathrm{i}\omega\mu(\sigma + \mathrm{i}\omega\varepsilon)}. \tag{5}$$

2.3 Method of moment (MoM)

Galerkin method is employed to solve the electric field integral equation in the frequency domain. The longitudinal current can be expanded as follows:

$$I(z) = \sum_{n=0}^{N} I_n F_n(z_n), \tag{6}$$

where $F_n(z_n)$ are the expansion functions and I_n denote the unknown coefficients to be determined. The sinusoidal current expansion is used as the basis and test functions in Galerkin method, and it is expressed as

$$\begin{cases} F_n = \dfrac{P_1(z)\sinh[\gamma(z - z_{n-1})]}{\sinh(\gamma\Delta z)} + \dfrac{P_2(z)\sinh[\gamma(z_{n+1} - z)]}{\sinh(\gamma\Delta z)}, \\ P_1(z) = \begin{cases} 1, & z_{n-1} < z < z_n, \\ 0, & \text{elsewhere}, \end{cases} \\ P_2(z) = \begin{cases} 1, & z_n < z < z_{n+1}, \\ 0, & \text{elsewhere}, \end{cases} \end{cases} \tag{7}$$

where $\Delta z = z_n - z_{n-1} = z_{n+1} - z_n$. The reason for the choice of the sinusoidal approximating function, Eq. (7), as the basis and test functions is that it is probably the only finite line source needed with simple closed-form expressions for the near fields. The rigorous expressions for the z-components of the electric field E_z and φ-components of the magnetic field H_φ at a near or distant point of a sinusoidal monopole of unit amplitude in a local cylindrical coordinate system illustrated in Fig. 2 are

$$E_z = \frac{1}{4\pi(\sigma + \mathrm{i}\omega\varepsilon)} \frac{\gamma}{\sinh(\gamma\Delta z)} \cdot \left\{ [I_1 - I_2\cosh(\gamma\Delta z)]\frac{\mathrm{e}^{-\gamma R_2}}{R_2} + [I_2 - I_1\cosh(\gamma\Delta z)]\frac{\mathrm{e}^{-\gamma R_1}}{R_1} \right\}, \tag{8}$$

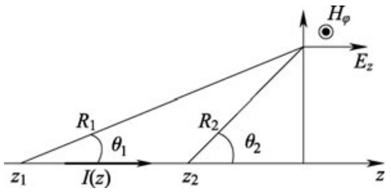

Fig. 2 Local coordinate system

$$H_\varphi = \frac{1}{4\pi\rho\sinh(\gamma\Delta z)}\{[I_1\sinh(\gamma\Delta z)\cos\theta_1 + I_1\cosh(\gamma\Delta z) - I_2]\mathrm{e}^{-\gamma R_1} - [I_2\sinh(\gamma\Delta z)\cos\theta_2 - I_2\cosh(\gamma\Delta z) + I_1]\mathrm{e}^{-\gamma R_2}\}, \tag{9}$$

where I_1 and I_2 are the values of monopole current $I(z)$, at z_1 and z_2, respectively,

$$I(z) = \frac{I_1\sinh[\gamma(z_2 - z)] + I_2\sinh[\gamma(z - z_1)]}{\sinh(\gamma\Delta z)}. \tag{10}$$

Using Eqs. (2) and (8), the linear algebraic equations can be obtained as follows:

$$\begin{bmatrix} z_{11} & z_{12} & \cdots & z_{1N} \\ z_{21} & z_{22} & \cdots & z_{2N} \\ \vdots & \vdots & & \vdots \\ z_{N1} & z_{N2} & \cdots & z_{NN} \end{bmatrix} \begin{bmatrix} I_1 \\ I_2 \\ \vdots \\ I_N \end{bmatrix} = \begin{bmatrix} -z_{10} \\ -z_{20} \\ \vdots \\ -z_{N0} \end{bmatrix}. \tag{11}$$

The dense form is

$$\boldsymbol{Z}_{N\times N}\boldsymbol{I}_{N\times 1} = \boldsymbol{U}_{N\times 1}, \tag{12}$$

where z_{mn} is the mutual impedance between dipoles m and n, z_{n0} is the mutual impedance between the dipole m and incident monopole, they can be expressed as follows:

$$\begin{aligned} z_{mn} &= \frac{1}{4\pi(\sigma + \mathrm{i}\omega\varepsilon)}\left[\int_{z_{m-1}}^{z_{m+1}} F_m(z,z_m) \cdot \int_{z_{n-1}}^{z_{n+1}} G(\boldsymbol{r}_m,\boldsymbol{r}_{1n}')F_n(z',z_n)\mathrm{d}z'\,\mathrm{d}z + a\int_{z_{m-1}}^{z_{m+1}} F_m(z,z_m) \cdot \int_{z_{n-1}}^{z_{n+1}} G(\boldsymbol{r}_m,\boldsymbol{r}_{2n}')F_n(z',z_n)\mathrm{d}z'\,\mathrm{d}z\right] \\ &= \int_{z_{m-1}}^{z_{m+1}} F_m(z,z_m)(E_{1zn} + aE_{2zn})\mathrm{d}z. \end{aligned} \tag{13}$$

2.4 Fast multipole method

Dividing the wire segments into M homogeneous groups, $\boldsymbol{o}$ and $\boldsymbol{o}_j'$ are the centers of groups $\boldsymbol{m}$ and $\boldsymbol{n}_j$, respectively. Applying FMM to Eq. (2), the linear algebraic equation, Eq. (12), can be rewritten as follows:

$$(\boldsymbol{Z}^{\mathrm{nearby}} + \boldsymbol{Z}^{\mathrm{far}})_{N\times N}\boldsymbol{I}_{N\times 1} = \boldsymbol{U}_{N\times 1}. \tag{14}$$

In the left hand side of Eq. (14), $\boldsymbol{Z}^{\mathrm{nearby}}$ represents the interaction from nearby regions, evaluated by Eq. (13), and $\boldsymbol{Z}^{\mathrm{far}}$ represents the interactions from non-nearby regions. For the non-nearby regions, by applying the addition theory, the exponential function is written as

$$\frac{\mathrm{e}^{-\gamma|\boldsymbol{r}-\boldsymbol{r}_j'|}}{|\boldsymbol{r}-\boldsymbol{r}_j'|} = \frac{\mathrm{e}^{-\mathrm{i}k|\boldsymbol{X}_j+\boldsymbol{d}_j|}}{|\boldsymbol{X}_j+\boldsymbol{d}_j|} \approx -\frac{\mathrm{i}k}{4\pi}\int \mathrm{e}^{-\mathrm{i}\boldsymbol{k}\cdot\boldsymbol{d}_j}T_j(\hat{\boldsymbol{k}}\cdot\hat{\boldsymbol{X}}_j)\mathrm{d}^2\hat{\boldsymbol{k}}, \tag{15}$$

where

$$\boldsymbol{X}_j = \boldsymbol{r}_{\boldsymbol{oo}_j'}, \tag{16}$$

$$\boldsymbol{d}_j = \boldsymbol{r}_{\boldsymbol{mo}} - \boldsymbol{r}_{\boldsymbol{n}_j\boldsymbol{o}_j'}, \tag{17}$$

$$\boldsymbol{r} - \boldsymbol{r}_j' = \boldsymbol{r}_{\boldsymbol{mn}_j} = \boldsymbol{X}_j + \boldsymbol{d}_j, \tag{18}$$

$$\boldsymbol{k} = k\hat{\boldsymbol{k}} = \frac{\gamma}{\mathrm{i}}\hat{\boldsymbol{k}}, \tag{19}$$

$$\hat{\boldsymbol{k}} = \sin\theta\cos\varphi + \sin\theta\sin\varphi + \cos\theta, \tag{20}$$

$$\int \mathrm{d}^2\hat{\boldsymbol{k}} = \int_0^{2\pi}\int_0^{\pi}\sin\theta\mathrm{d}\theta\mathrm{d}\varphi, \tag{21}$$

$$T_j(\hat{\boldsymbol{k}}\cdot\hat{\boldsymbol{X}}_j) = \sum_{l=0}^{L}(-\mathrm{i})^l(2l+1)h_l^{(2)}(kX_j)P_l(\hat{\boldsymbol{k}}\cdot\hat{\boldsymbol{X}}_j), \tag{22}$$

$$L = kD + 2\ln(kD + \pi), \tag{23}$$

where $\int \mathrm{d}^2\hat{\boldsymbol{k}}$ is the integral over the unit sphere, $h_l^{(2)}$ is a spherical Hankel function of the second kind, P_l is a Legendre polynomial, and $d_j < X_j$. D is the maximum group size. When using this expansion to compute the field at $\boldsymbol{m}$ from a source at $\boldsymbol{n}_j$, $\boldsymbol{X}_j$ will be chosen to be close to $\boldsymbol{m} - \boldsymbol{n}_j$, so that d_j will be small. This relationship of the various vectors is sketched in Fig. 3.

Furthermore,

$$\begin{aligned} G(\boldsymbol{r},\boldsymbol{r}_j') &= (\nabla^2 - \gamma^2)\frac{\mathrm{e}^{-\gamma|\boldsymbol{r}-\boldsymbol{r}_j'|}}{|\boldsymbol{r}-\boldsymbol{r}_j'|} \\ &\approx -\frac{\mathrm{i}k}{4\pi}\int(\nabla^2 - \gamma^2)\mathrm{e}^{-\mathrm{i}\boldsymbol{k}\cdot\boldsymbol{d}_j}T_j(\hat{\boldsymbol{k}}\cdot\hat{\boldsymbol{r}}_j)\mathrm{d}^2\hat{\boldsymbol{k}} \\ &= -\frac{\gamma^3}{4\pi}\int \mathrm{e}^{-\mathrm{i}\boldsymbol{k}\cdot\boldsymbol{d}_j}T_j(\hat{\boldsymbol{k}}\cdot\hat{\boldsymbol{r}}_j)(\cos^2\theta - 1)\mathrm{d}^2\hat{\boldsymbol{k}}, \end{aligned} \tag{24}$$

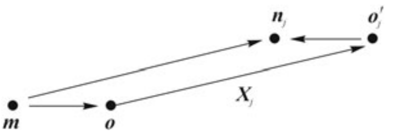

Fig. 3 Relationship between locations $\boldsymbol{m}$ and $\boldsymbol{n}_j$

$$
\begin{aligned}
z_{mn}^{\text{far}} &= \frac{1}{4\pi(\sigma+\mathrm{i}\omega\varepsilon)}\int_{z_{m-1}}^{z_{m+1}}\int_{z_{n-1}}^{z_{n+1}}[F_m(z,z_m)G(\boldsymbol{r},\boldsymbol{r}_1')F_n(z',z_n) \\
&\quad + aF_m(z,z_m)G(\boldsymbol{r},\boldsymbol{r}_2')F_n(z',z_n)]\mathrm{d}z\mathrm{d}z' \\
&= -\frac{\gamma^3}{16\pi^2(\sigma+\mathrm{i}\omega\varepsilon)}\int V_m\left[T_1\left(\hat{\boldsymbol{k}}\cdot\hat{\boldsymbol{r}}_1\right)+aT_2\left(\hat{\boldsymbol{k}}\cdot\hat{\boldsymbol{r}}_2\right)\right] \\
&\quad \cdot\left(\cos^2\theta-1\right)V_n\mathrm{d}^2\hat{\boldsymbol{k}},
\end{aligned} \tag{25}
$$

where

$$
V_m = \int_{z_{m-1}}^{z_{m+1}} F_m(z,z_m)\mathrm{e}^{-\mathrm{i}\boldsymbol{k}\cdot\boldsymbol{r}_{mo}}\mathrm{d}z, \tag{26}
$$

$$
\begin{aligned}
V_n &= \int_{z_{n_1-1}}^{z_{n_1+1}} F_{n_1}(z',z_{n_1})\mathrm{e}^{\mathrm{i}\boldsymbol{k}\cdot\boldsymbol{r}_{n_1o_1'}}\,\mathrm{d}z' \\
&= \int_{z_{n_2-1}}^{z_{n_2+1}} F_{n_2}(z',z_{n_2})\mathrm{e}^{\mathrm{i}\boldsymbol{k}\cdot\boldsymbol{r}_{n_2o_2'}}\,\mathrm{d}z',
\end{aligned} \tag{27}
$$

where T_j, V_m, V_n represent the matrix of translation, aggregation, and disaggregation, respectively. Because the wire is divided symmetrical, T_j has a translational invariance, and for the elements in different groups, when $\boldsymbol{r}_{mo}$ is equal, V_m is equal, V_n also has the same nature. Furthermore, V_m and V_n are unchanged for the current source and its image, and these properties reduce the computational complexity and computer memory significantly.

3 Numerical results

In order to examine the validity of the developed algorithm, we computed the longitudinal current along the wire in Fig. 1, where $L = 40$ m, $\sigma = 0.0005$ mho/m, $\mu_r = 1$, and $\varepsilon_r = 4$. It is assumed that the wire is excited at its far-left side (point s in Fig. 1) by a sinusoidal current with unit amplitude of frequency $f = 6.741$ MHz. Figures 4, 5 and 6 show the current distribution along the wire, x-component of the electric field along the z-axis and y-component of magnetic field along the z-axis, respectively, calculated by the algorithm developed based on FMM in this paper and by MoM directly. It can be found that a good agreement has been achieved between the two methods. In order to show the efficiency of the method developed in this paper, we separately used the MoM, FMM (group number $M = 4$) and FMM (group number $M = 7$) to solve

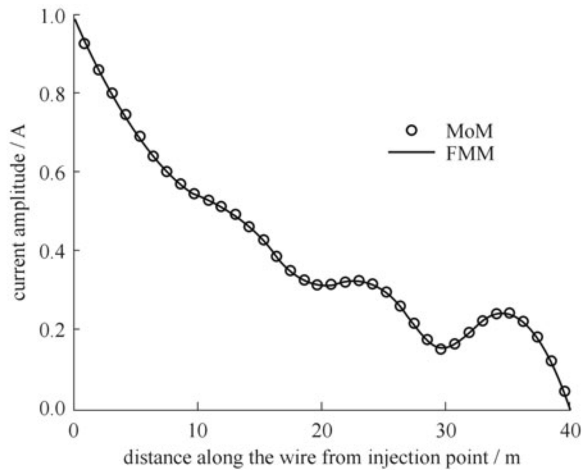

Fig. 4 Current distribution along the wire

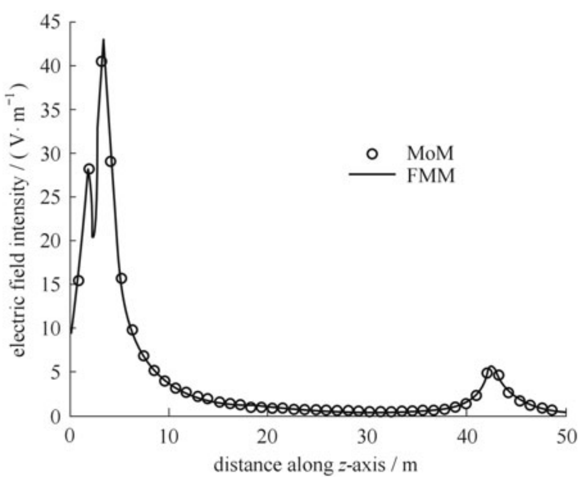

Fig. 5 x-component of electric field along z-axis

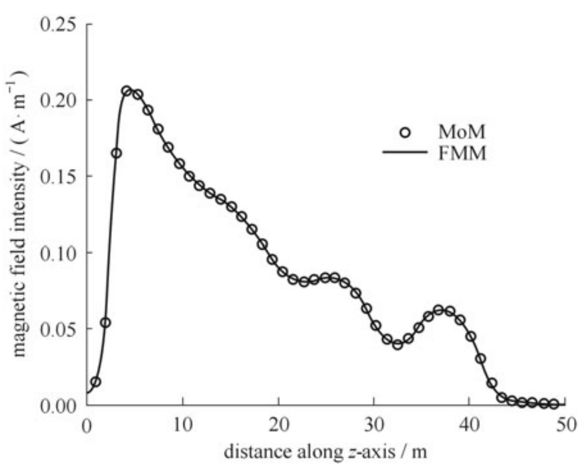

Fig. 6 y-component of magnetic field along z-axis

the EFIE with a different number of unknowns, and the operation time is given in Fig. 7. It is clear from Fig. 7 that the more the groups are, the faster the solution is, and the more the unknowns to be solved, the more obvious the superiority of FMM over MoM. Therefore, the algorithm developed based on FMM in this paper is more suitable to calculate the transient characteristic of grounding grid of a large substation when it is stricken by lightning.

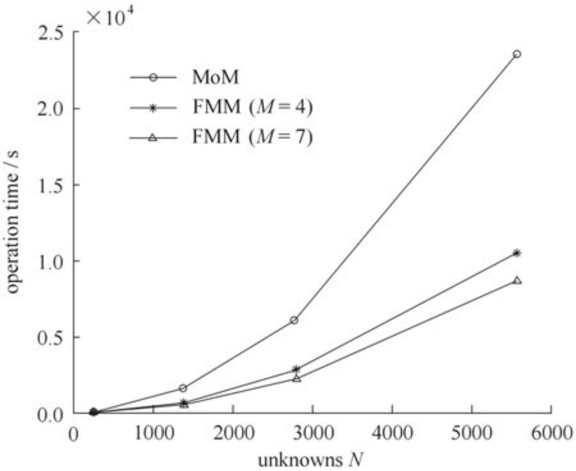

Fig. 7 Operation time

4 Conclusion

A fast algorithm is presented to compute the electromagnetic field of thin wire current source inside a lossy ground. The method used the modified images to replace the ground effect, and utilized the fast multipole method for solving the governing electric field integral equation. The method is capable of modeling end-point charges representing the excitation point of the wire, and it also can be used in analyzing lightning electromagnetic field problems of substation grounding systems or overhead transmission lines.

Acknowledgements This work was supported by the National Natural Science Foundation of China (Grant No. 50577019) and in part by the Natural Science Foundation of Hebei Province (No. E2006000678).

References

1. Rachidi F, Ianoz M, Nucci C A, Mazzetti C. Calculation methods of the horizontal component of lightning return stroke electric fields. In: Proceedings of the 11th International Wroclaw Symposium on Electromagnetic compatibility. 1992, 452–456
2. Cooray V. Horizontal fields generated by return strokes. Radio Science, 1992, 27(4): 529–537
3. Rubinstein M. An approximate formula for the calculation of the horizontal electric field from lightning at close, intermediate, and long range. IEEE Transactions on Electromagnetic Compatibility, 1996, 38(3): 531–535
4. Cooray V. Some considerations on the "Cooray-Rubinstein" formulation used in deriving the horizontal electric field of lightning return strokes over finitely conducting ground. IEEE Transactions on Electromagnetic Compatibility, 2002, 44(4): 560–566
5. Cooray V. On the accuracy of several approximate theories used in quantifying the propagation effects on lightning generated electromagnetic fields. IEEE Transactions on Antennas and Propagation, 2008, 56(7): 1960–1967
6. Delfino F, Procopio R, Rossi M, Rachidi F, Nucci C A. An algorithm for the exact evaluation of the underground lightning electromagnetic fields. IEEE Transactions on Electromagnetic Compatibility, 2007, 49(2): 401–411
7. Coifman R, Rokhlin V, Wandzura S. The fast multipole method for the wave equation: a pedestrian prescription. IEEE Antennas and Propagation Magazine, 1993, 35(3): 7–12
8. Eibert T F. A diagonalized multilevel fast multipole method with spherical harmonics expansion of the k-space integrals. IEEE Transactions on Antennas and Propagation, 2005, 53(2): 814–817
9. Hu J, Nie Z P, Lei L, Rui X, Wang J. Solving 3D electromagnetic scattering and radiation by local multilevel fast multipole algorithm. Chinese Journal of Electronics, 2007, 16(2): 366–369
10. Grcev L D. Computer analysis of transient voltages in large grounding systems. IEEE Transactions on Power Delivery, 1996, 11 (2): 815–823